jmb

Neuronatin Is Associated with an Anti-Inflammatory Role in the White Adipose Tissue

Hye In Ka, Sora Han, Ae Lee Jeong, Sunyi Lee, Hyo Jeong Yong, Ariundavaa Boldbaatar, Hyun Jeong Joo, Su Jung Soh, Ji Young Park, Jong-Seok Lim, Myung Sok Lee, and Young Yang*

Department of Biological Sciences, Sookmyung Women's University, Seoul 04310, Republic of Korea

Neuronatin (NNAT) is known to regulate ion channels during brain development and plays a role in maintaining the structure of the nervous system. A previous in silico analysis showed that *Nnat* was overexpressed in the adipose tissue of an obese rodent model relative to the wild type. Therefore, the aim of the present study was to investigate the function of *Nnat* in the adipose tissue. Because obesity is known to systemically induce low-grade inflammation, the *Nnat* expression level was examined in the adipose tissue obtained from C57BL/6 mice administered lipopolysaccharide (LPS). Unexpectedly, the *Nnat* expression level decreased in the white adipose tissue after LPS administration. To determine the role of NNAT in inflammation, 3T3-L1 cells overexpressing *Nnat* were treated with LPS. The level of the p65 subunit of nuclear factor-kappa B (NF-κB) and the activity of NF-κB luciferase decreased following LPS treatment. These results indicate that NNAT plays an anti-inflammatory role in the adipose tissue.

Keywords: Adipocyte, anti-inflammation, inflammation, NF-κB, neuronatin, obesity

Introduction

Obesity is the main cause of the metabolic syndrome associated with insulin resistance, type 2 diabetes [1], cardiovascular disease, and cancer [2, 3], and all of these diseases are also related to inflammation [4]. Because obesity can induce systemic low-grade chronic inflammation, several studies have evaluated the relationship between obesity and inflammation [4–6]. Many inflammatory genes showing expression differences between lean and obese individuals have been identified, and the contributions of inflammatory genes, including those encoding tumor necrosis factor-alpha (TNF-α), interleukin-6, monocyte chemotactic protein-1 (MCP-1), inducible nitric oxide synthase, and adiponectin (APN), have been studied using mice with null mutations [7–9]. However, the causal link of these inflammatory genes to particular metabolic outcomes remains unclear. In this regard, the identification and functional analysis of the gene clusters involved in adipose-induced inflammation should be examined to understand the mechanisms of the genes involved in metabolic disease.

Neuronatin (*Nnat*), which was first identified as a paternally expressed imprinted gene [10, 11], has two splicing variant forms. *Nnat α* is composed of three exons and is alternatively spliced to produce *Nnat β* [12]. *Nnat β* does not contain a middle exon encoding a part of the membrane domain, but remains localized to the endoplasmic reticulum (ER), similar to NNAT α [13]. The expression of each isoform differs depending on the tissue or cellular homeostatic status. NNAT is expressed in the hypothalamic nuclei and is related to nutrient sensing and feeding/fasting [14]. In addition to the metabolism-related function of NNAT in the brain, this protein has also been associated with insulin function. NNAT co-localizes with insulin in pancreatic β-cells, and the depletion of NNAT leads to a dramatic reduction in glucose-mediated insulin secretion [15]. In addition, NNAT β has been reported to play a critical role in the pathogenesis of type 2 diabetes by mediating the high glucose-induced apoptosis of pancreatic β-cells [16]. NNAT also plays a role in adipocyte differentiation by increasing the intracellular Ca^{2+} level through the regulation of Ca^{2+}ATPase in the ER [17].

Although the functional relationship of NNAT in metabolism has been evaluated in several studies, its function in the adipose tissue remains unexplored. In this study, a set of genes with expression specific to the white adipose tissue and up-regulated in high-fat diet-fed mice was identified using in silico analysis. The function of NNAT in the adipose tissue was further evaluated to clarify its role in adipocytes.

Materials and Methods

Cell Culture and Transfection

Both 3T3-L1 preadipocytes (American Type Culture Collection, USA) and HEK293T cells were cultured in Dulbecco's modified Eagle's medium (DMEM) supplemented with 10% heat-inactivated fetal bovine serum (HyClone, USA) in a humidified chamber with 5% CO_2 at 37°C. The HEK293T and 3T3-L1 cells were transfected directly with plasmid DNA using Lipofectamine2000 Plus reagent (Invitrogen, USA) according to the manufacturer's protocol.

Animals

We used 6-week-old male C57BL/6 mice and *db/db* obese mice purchased from the Jackson Laboratory. Bedding was changed once a week and the temperature and humidity were controlled. Mice were housed under 12-h light/12-h dark conditions and allowed free access to food and water. The plans and protocols for the animal experiments were approved by the Institutional Animal Care and Use Committee of Sookmyung Women's University, Seoul, Republic of Korea (SMWU-IACUC-1508-014).

Differentiation of 3T3-L1 Cells

When the 3T3-L1 cells reached confluence, they were induced to differentiate by changing the medium to a differentiation medium (DMEM containing 1 μg/ml of insulin, 0.25 μM dexamethasone, 0.5 mM 3-isobutyl-1-methylxanthine, and 10% fetal bovine serum) and cultured for 2 days. The cells were then maintained in differentiation maintenance medium (DMEM containing 1 μg/ml of insulin and 10% fetal bovine serum). The differentiation maintenance medium was changed every other day until the cells were harvested.

Stromal-Vascular Cell Fraction

The C57BL/6 mice were administered 1 μg/ml lipopolysaccharide (LPS), and epididymal fat tissues were obtained. The tissues were minced and incubated at 37°C for 20 min in phosphate-buffered saline (PBS) containing 0.75 mg/ml of type 2 collagenase (Worthington Biochemical Corp., USA). The lipid layer (top layer) and the stromal-vascular cell fraction (SVF; pellets) were collected after centrifugation at 18,000 ×*g* for 3 min, and total RNA was isolated for reverse transcription-polymerase chain reaction (RT-PCR) analysis.

Antibodies and Chemicals

The following primary antibodies were used: anti-NNAT (ab27266; Abcam, UK), anti-β-actin (sc-4778; Santa Cruz Biotechnology, USA), anti-IκBα (4814; Cell Signaling, USA), anti-p65 (8242; Cell Signaling), and anti-phospho-p65 antibody (3033; Cell Signaling). Dexamethasone, 3-isobutyl-1-methylxanthine, insulin, and LPS (L2880) were purchased from Sigma-Aldrich (USA).

Cloning and Plasmid Construction

Mouse cDNAs of *Nnat α* and *Nnat β* were generated by PCR, sequenced, and then subcloned into the EcoRI-SalI sites of the pEGFP-C2 mammalian expression plasmid. Mouse cDNAs of *p65* were subcloned into the EcoRI-HindIII sites of the pCMV-Tag2B mammalian expression plasmid.

Immunoblot Assay

Cell lysates were mixed with 5× sodium dodecyl sulfate (SDS) sample buffer and heated at 95°C for 5 min. The proteins were separated electrophoretically on a 10% SDS-polyacrylamide gel and transferred onto a 0.45-μm-pore-size nitrocellulose membrane (GE Healthcare, UK) for 2 h. The membrane was incubated overnight with primary antibodies at 4°C, followed by incubation with horseradish peroxidase-conjugated goat anti-mouse or anti-rabbit IgG (Fab) secondary antibodies (Enzo Life Sciences, USA) at room temperature for 2 h. The proteins were visualized using PowerOpti-ECL western blotting reagent (Animal Genetics, Korea) and analyzed using an LAS3000 luminescent image analyzer (Fuji Film, Japan).

Subcellular Localization

The 3T3-L1 cells ($1 × 10^5$ cells) were seeded onto glass coverslips in 12-well plates and transfected with the NNAT-green fluorescent protein (GFP) expression plasmid. After incubation for 24 h, the cells were fixed with 4% formaldehyde for 15 min, washed with PBS, and then permeabilized with 0.1% Triton X-100 at 22°C for 10 min. After washing with PBS, the cells were blocked with 3% bovine serum albumin at 22°C for 15 min, and then stained with DAPI mounting medium (Sigma-Aldrich). Images were acquired using an AxioVision 4.8.2 (Carl Zeiss, Germany) system under a Zeiss Axiovert 200 m microscope, using a 1.4 numerical aperture plan-Apo ×63 oil immersion lens and a HRm charge-coupled device camera.

RT-PCR

Total RNA samples of cells and tissues were prepared using RNAiso-plus (Takara, Japan) according to the manufacturer's protocol. The isolated total RNA was reverse-transcribed using M-MuLV reverse transcriptase (Promega, USA) at 37°C for 1 h. The PCR primer sequences used in this study are all listed in Table 1. The RT-PCR products were visualized by 1% agarose gel electrophoresis, and the intensity of the bands was measured using a DNR Bio-Imaging system (Kiryat Anavim, Israel).

Table 1. Primer sequences for RT-PCR.

Gene	Forward primer (5′-3′)	Reverse primer (5′-3′)
Nnat α	GAACCCTTGCTCTCGACCAC	CTGAACACCTCACTTCTCGCA
Nnat β	GTGCTGCTGCAGGTGTTCAG	TACGCCCATATCTCGAGGT
Mcp-1	ATCCCAATGAGTAGGCTGGAGAGC	CAGAAGTGCTTGAGGTGGTTGTG
Pai-1	GCCAGATTTATCATCAATGACTGGG	GGAGAGGTGCACATCTTTCTCAAAG
Il-1β	TGCCACCTTTTGACAGTGATG	CATCTCGGAGCCTGTAGTGC
Tnf-α	CGAGTGACAAGCCTGTAGC	CCCTTCTCCAGCTGGAAGAC
Apn	TGGTGAGAAGGGTGAGAA	AGATCTTGGTAAAGCGAATG
β-Actin	CTTCCTGCAAGAGTATGTCACG	TGGAGGTGAGATGGTGACTG

Luciferase Assay

HEK293T cells and 3T3-L1 cells were seeded into 12-well plates and allowed to adhere for 24 h. The cells were then co-transfected with a mixture of 200 ng pCS5-3XFlag-p65 plasmid, 200 ng pGL3-4xNF-κB-luciferase reporter plasmid, 5 ng pRL-CMV plasmid, and 200 ng pEGFP-C2-NNATα or β plasmid using Lipofectamine 2000 reagent. After LPS treatment, the cells were lysed, and luciferase activity was determined using the Dual-Luciferase Reporter Assay System (Promega) according to the manufacturer instructions.

Statistical Analysis

Values are presented as the mean ± standard deviation (SD). Multiple comparisons within groups were made with one-way analysis of variance (ANOVA), and individual group mean differences were evaluated using the Student's *t*-test. A maximum level of significance of $p < 0.05$ was used for all statistical comparisons. All statistical analyses were performed using GraphPad Prism ver. 5.0 for Windows (GraphPad Software, USA; http://www.graphpad.com).

Results

Nnat mRNA Expression Is Relatively Specific in White Adipose Tissue and Highly Expressed in the White Adipose Tissue of High-Fat Diet-Fed Mice

To select genes that were highly and specifically expressed in the white adipose tissue from high-fat diet-fed mice compared with low-fat diet-fed mice, two different microarray gene expression datasets were analyzed using the Gene Expression Omnibus (http://www.ncbi.nlm.nih.gov/geo/) of the National Center for Biotechnology Information. First, to identify the genes differentially expressed in the white adipose tissue of high-fat diet-fed mice compared with low-fat diet-fed mice, GSE38337 was analyzed. As a result, 81 genes were defined as significantly differentially expressed, showing $p < 0.01$ and |log2 (fold change)|> 1 average values between the two diet groups. Next, to select genes that were specifically expressed in the

Table 2. List of common genes between those with more than | log2 (fold-change) | > 1 expression changes in adipose tissue of high-fat diet-fed mice and those specific to white adipose tissue.

Gene name	Gene symbol
Neuronatin	*Nnat*
Leptin	*Lep*
Interferon, alpha-inducible protein 27 like 2A	*Ifi27l2a*
Stearoyl-coenzyme A desaturase 1	*Scd1*
Pyruvate carboxylase	*Pcx*
1-Acylglycerol-3-phosphate *O*-acyltransferase 2	*Agpat2*
Fatty acid synthase	*Fasn*
Solute carrier family 36 (proton/amino acid symporter), member 2	*Slc36a2*
Solute carrier family 25 (mitochondrial carrier, citrate transporter), member 1	*Slc25a1*
Claudin 22	*Cldn22*
Prostate transmembrane protein, androgen induced 1	*Pmepa1*
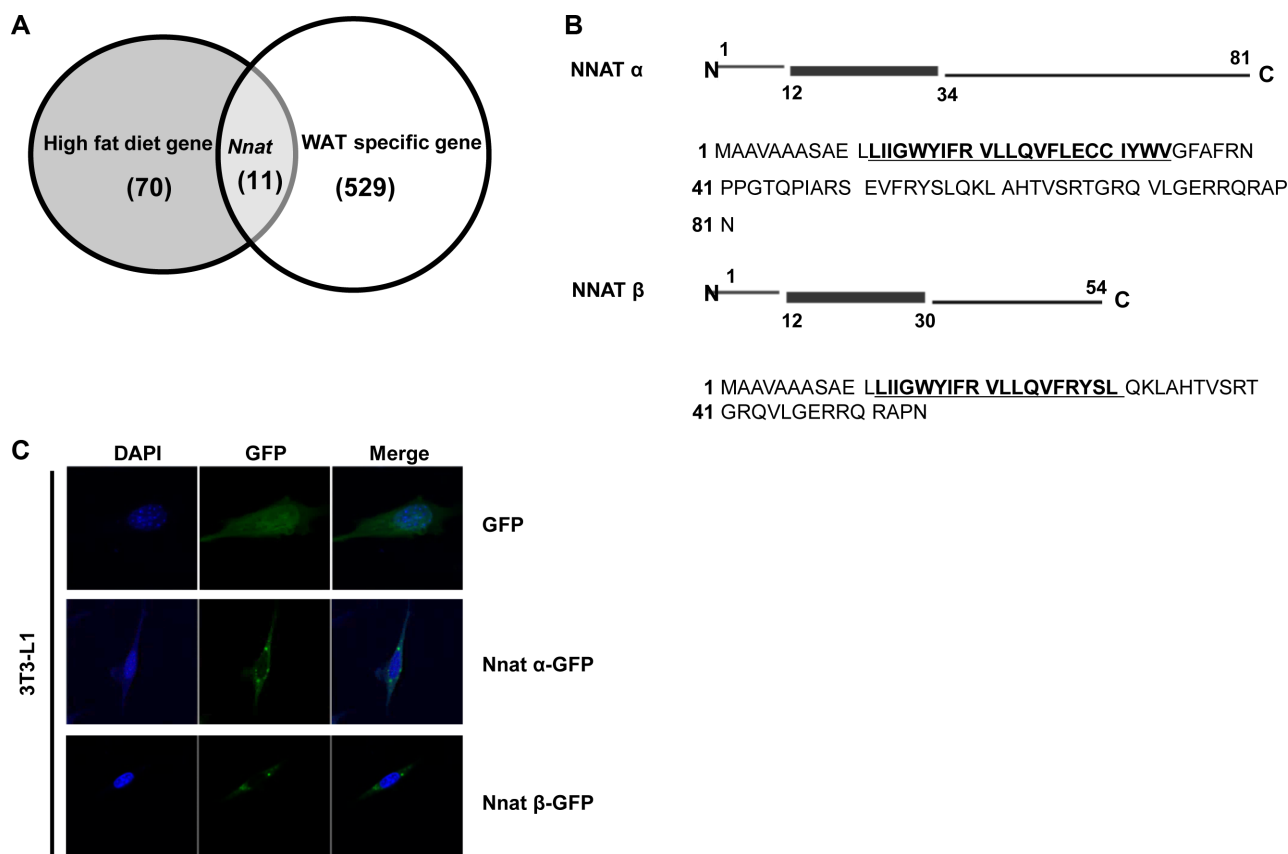
Fig. 1. Analysis of *Nnat* expression in the white adipose tissue of high-fat diet-fed mice and localization in the 3T3-L1 cells. (**A**) Venn diagram showing common genes with more than 2-fold expression changes in the white adipose tissue of high-fat diet-fed mice and genes showing specific expression in the white adipose tissue compared with other tissues. (**B**) NNAT α and NNAT β protein domains were predicted on the basis of TMHMM database analysis. Black thick lines and underlined sequences indicate putative transmembrane domains. The NNAT α transmembrane helix contains 23 amino acids, and NNAT β contains 19 amino acids. N, N-terminus; C, C-terminus. (C) The 3T3-L1 cells were transfected with Nnat α-GFP and Nnat β-GFP expression plasmids and then fixed and stained with DAPI after 24-h incubation.

white adipose tissue among a variety of tissues, GSE9954 was analyzed, and 540 genes were identified as being relatively highly expressed in the white adipose tissue. Finally, common genes, which satisfied both conditions, were extracted, and 11 genes were identified (Fig. 1A). The list of genes is summarized in Table 2. Among these genes, the leptin and fatty acid synthase genes are well known to be significantly related to obesity [18−20]. Although *Nnat* was highly ranked as a positively expressed gene in the common genes group, little is known regarding its role in the adipose tissue.

To determine the role of NNAT, the localization of NNAT α and NNAT β was estimated using TMHMM, a program for the prediction of transmembrane helices based on a hidden Markov model [21]. This analysis revealed that NNAT α had a type I transmembrane helix consisting of 23 amino acids, and NNAT β comprised 19 amino acids

(Fig. 1B). Cells of the preadipocyte cell line 3T3-L1 were transfected with the *Nnat* α and *Nnat* β expression vectors, and both genes showed similar cytosolic and dot localization patterns (Fig. 1C).

Nnat β Expression Is Increased in the White Adipose Tissue of *db/db* Mice But No Significant Difference Was Observed during Adipocyte Differentiation

To confirm the in silico results, *Nnat β* expression levels were examined using RT-PCR analysis in the adipose tissue of wild-type and *db/db* obese mice because it is known that *Nnat α* expression is increased in 3T3-L1 cells [17]. *Nnat β* expression was also significantly increased in the adipose tissue of *db/db* mice, similar to *Nnat α* expression. When the *Nnat β* band intensity was normalized to that of β-actin, the level was found to be increased by approximately 3-fold compared with that of wild-type

A

B

C
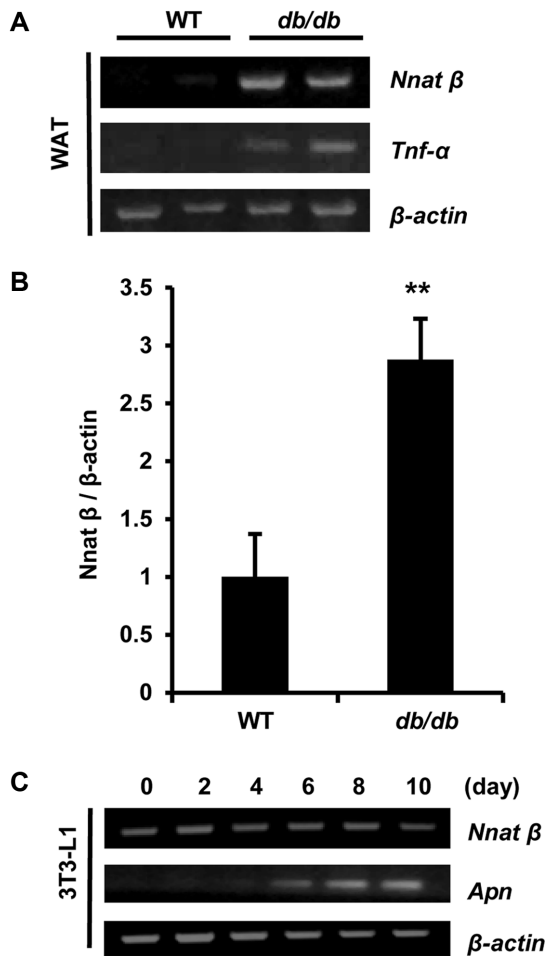
Fig. 2. Relative mRNA expression of *Nnat β* in the white adipose tissue of *db/db* mice, and differentiated adipocytes. (**A**) *Nnat β* mRNA expression levels in the white adipose tissue of wild-type and *db/db* mice were examined by RT-PCR. (**B**) The results of (**A**) were graphed after determining the intensities of *Nnat β* expression normalized by β-actin using Gelquant software. **, $p < 0.01$, one-tailed Student's *t*-test. (**C**) *Nnat β* and adiponectin (*Apn*) mRNA expression levels in the 3T3-L1 cells induced to differentiate for 10 days were analyzed by RT-PCR.

mice (Figs. 2A and 2B). Next, to determine whether the adipose tissue of *db/db* mice is in an inflammatory state, the TNF-α expression level, as a proinflammatory gene marker, was examined. The levels were increased in the adipose tissue of *db/db* mice (Fig. 2A), indicating that the *Nnat β* expression level is increased in inflammatory adipose tissue.

Next, to examine whether *Nnat β* expression is associated with adipogenesis, similar to *Nnat α* [17], 3T3-L1 preadipocytes were differentiated by treatment with a differentiation cocktail. The cells were harvested every 2 days after the beginning of differentiation, and the *Nnat β* expression

level was examined by RT-PCR. The levels of the well-known differentiation marker *Apn* gradually increased with differentiation. However, no significant difference in the *Nnat β* level was observed, regardless of the differentiation status (Fig. 2C).

Nnat α and *Nnat β* Expression Decreased in the White Adipose Tissue Following LPS Treatment

Because obesity is known to systemically induce low-grade inflammation, and *Nnat* expression is increased in the adipose tissue of obese mice, we hypothesized that *Nnat* expression may be increased by obesity-induced inflammatory stimuli. To test this possibility, wild-type mice were intraperitoneally administered with 1 μg/ml LPS, and the white adipose tissue was harvested for the measurement of *Nnat* levels. Unexpectedly, the RT-PCR results showed that *Nnat α* and *Nnat β* levels in the white adipose tissue of LPS-administered mice were significantly lower than those in vehicle-administered wild-type mice (Fig. 3). These results indicate that an inflammatory stimulus reduces *Nnat α* and *Nnatβ* expression, in contrast to our expectation.

LPS Treatment Reduces *Nnat α* and *Nnat β* Expression in the Adipocytes

To determine which cells are responsible for causing the observed decrease in *Nnat* expression levels following LPS treatment, the white adipose tissue extracted from mice administered 1 μg/ml LPS for 3 h was fractionated into adipocytes and an SVF, as the white adipose tissue contains not only adipocytes but also stromal-vascular cells, including fibroblasts, macrophages, and preadipocytes. *Nnat α* was expressed in both the adipocytes and SVF, whereas *Nnat β* was mainly expressed in the adipocytes. Both *Nnat* isoforms were dramatically decreased in the adipocytes of LPS-administered mice, whereas the levels of proinflammatory cytokines *Il-1β* and *Pai-1* and the chemokine *Mcp-1* were enhanced by LPS administration (Fig. 4A).

Next, to examine whether *Nnat* expression is also decreased by LPS treatment in vitro, differentiated 3T3-L1 cells were treated with 1 μg/ml of LPS for the indicated times. *Nnat α* and *Nnat β* expression levels also decreased time-dependently, whereas *Mcp-1* was increased at the early time points of LPS treatment (Fig. 4B). This result indicates that LPS treatment decreases *Nnat* expression in adipocytes.

NNAT α and NNAT β Inhibit Expression of the p65 Subunit of NF-κB in Adipocytes

Although a high level of *Nnat* was expected in LPS-
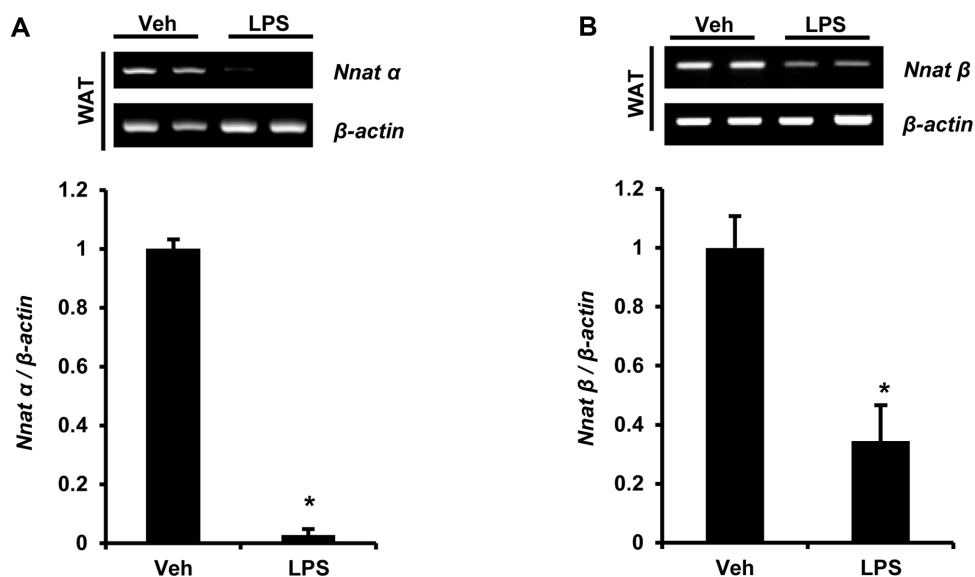
Fig. 3. Relative mRNA expression of *Nnat α* and *Nnat β* in the white adipose tissue following lipopolysaccharide (LPS) treatment. (**A**, **B**) Wild-type mice were administered 1 μg/ml of LPS, and the white adipose tissue was extracted for analysis of *Nnat α* (**A**) and *Nnat β* (**B**) mRNA expression levels by RT-PCR. The intensities of *Nnat α* and *Nnat β* expression normalized to β-actin using Gelquant software were graphed. *, $p < 0.05$, one-tailed Student's *t*-test.
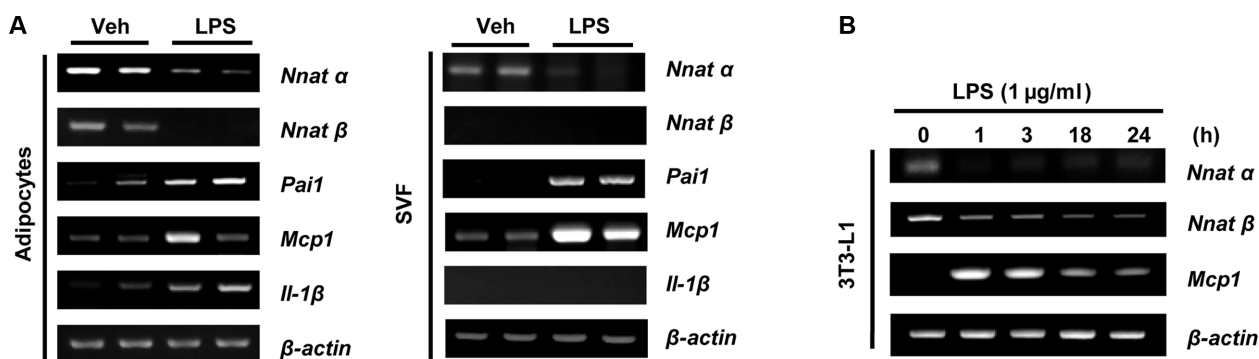

Fig. 4. Relative mRNA expression of *Nnat α, Nnat β,* and proinflammatory genes in adipocytes and the stromal-vascular cell fraction (SVF) following lipopolysaccharide (LPS) treatment.
(**A**) Wild-type mice were administered 1 μg/ml of LPS for 3 h, and the extracted epididymal fat pads were separated into adipocytes and SVF. The mRNA expression levels of *Nnat α, Nnat β,* and proinflammatory genes were analyzed by RT-PCR. (**B**) The 3T3-L1 cells differentiated for 10 days were treated with 1 μg/ml of LPS for the indicated times, and *Nnat* mRNA levels were analyzed by RT-PCR.

administered mice because it is increased in a condition of low-grade inflammation such as obesity, LPS-administered mice unexpectedly showed decreased *Nnat* expression in adipose tissue. Thus, the role of NNAT in inflammatory signaling pathways was unclear. Because the inflammatory signal is mediated by the NF-κB signaling pathway [22] and a previous study proposed that NNAT expression leads to activation of NF-κB in aortic endothelial cells [23], we evaluated whether NNAT expression is associated with NF-κB activation in adipocytes. Thus, 3T3-L1 cells were co-

transfected with an NF-κB luciferase vector together with a plasmid expressing NNAT α or β, respectively. Co-transfection with p65 increased NF-κB luciferase activity, whereas NNAT α reduced the luciferase activity by approximately 2-fold. Co-transfection with NNAT β also inhibited luciferase activity but showed a lower reducing efficiency than that observed with NNAT α (Fig. 5A). These results indicate that NNAT α and NNAT β have anti-inflammatory functions, and the anti-inflammatory ability of NNAT α is stronger than that of NNAT β.

A

B
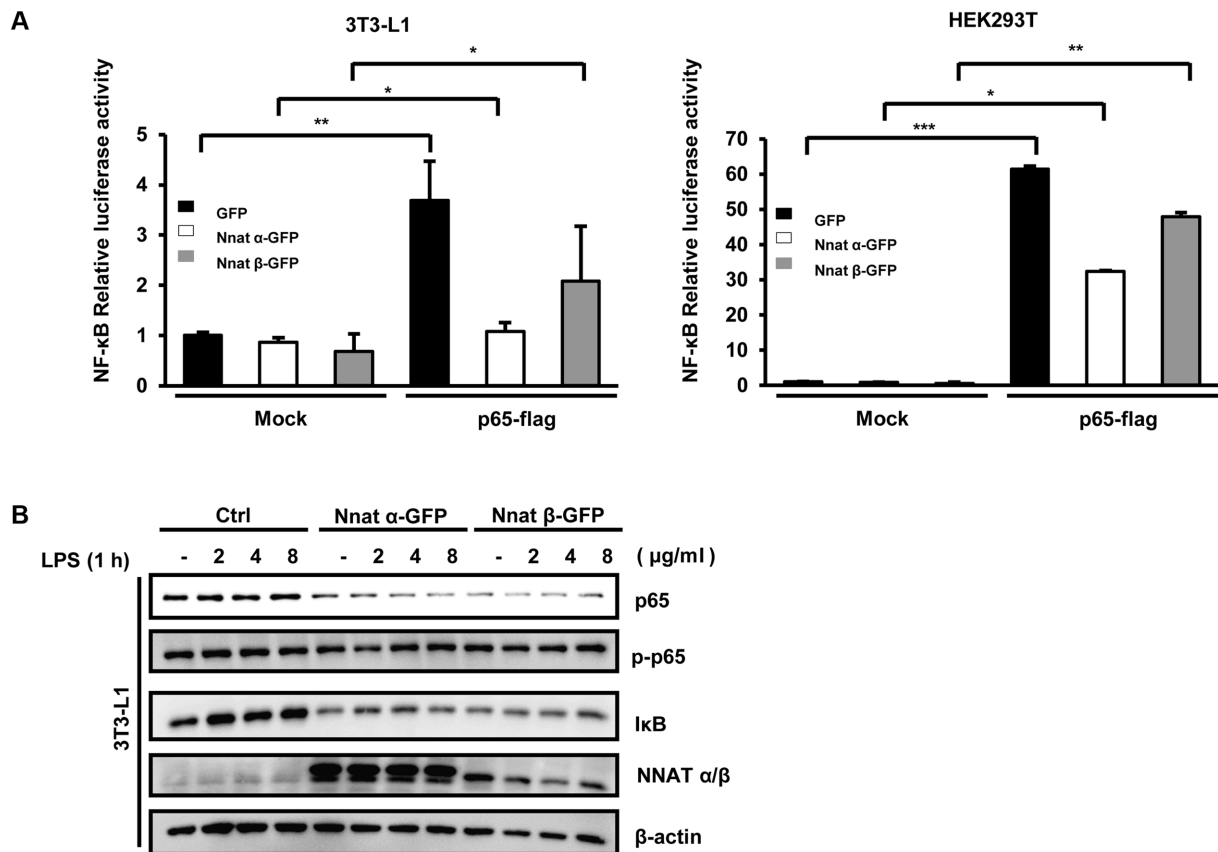
Fig. 5. Effects of NNAT α and NNAT β on NF-κB activity in adipocytes.

(**A**) The 3T3-L1 and HEK293T cells were transfected with the NF-κB luciferase plasmid, FLAG-p65 expression plasmid, and NNAT α-GFP or NNAT β-GFP expression plasmid; the relative luciferase activity was analyzed 1 day after transfection. Firefly luciferase was used as a reporter, and *Renilla* luciferase was used as a control. The results of three independent experiments are shown. *, $p < 0.05$; **, $p < 0.01$; ***, $p < 0.001$, two-tailed ANOVA. (**B**) The 3T3-L1 cells were transfected with NNAT α-GFP or NNAT β-GFP for 24 h, and harvested 1 h after treatment with 1 μg/ml lipopolysaccharide (LPS). The expression levels of p65, p-p65, IκB, and NNAT α/β were analyzed by immunoblot assay. β-Actin served as the loading control.

Next, to further examine whether NNAT affects the expression of the p65 subunit of NF-κB, 3T3-L1 cells were transfected with either the GFP-control or NNAT-GFP plasmid, followed by treatment with different doses of LPS. Immunoblot analysis showed that p65 expression was remarkably inhibited upon LPS treatment in 3T3-L1 cells overexpressing NNAT compared with control cells (Fig. 5B). Thus, NNAT has an anti-inflammatory role in adipocytes.

Discussion

Transcriptome analysis is very useful for identifying a group of new candidate genes regulated in a specific condition. In the present study, we searched for a set of common genes showing significant expression differences in the white adipose tissue of high-fat diet-fed mice and

that were relatively specifically expressed in the white adipose tissue compared with other tissues of wild-type mice. Among the genes identified, leptin is well known as a key hormone marker for obesity, is secreted by adipocytes [18, 19], and regulates energy homeostasis by controlling appetite in both humans and rodents. Pyruvate carboxylase (*Pcx*) expression is also increased in rodent models of type 1 diabetes [24, 25] and in obese Zucker diabetic fatty rats [26], and *Pcx* is known to be involved in gluconeogenesis and hepatic glucose production [25]. Therefore, our strategy for identifying gene sets was confirmed to be efficient. Although *Nnat* is known to be mainly expressed in the brain of normal mice, *Nnat* ranked highest for expression in the adipose tissue in this study. This may be because of the relatively dramatic increase of *Nnat* in the adipose tissue of obese rodent models

compared with wild-type mice.

Because obesity systemically induces chronic low-grade inflammation and *Nnat* expression is increased in obese rodent models, we expected that LPS treatment, as an inflammatory stimulus, would increase the level of *Nnat* expression; however, *Nnat α* and *Nnat β* mRNA expression levels were decreased following LPS treatment. This may be related to the different responses to acute and chronic inflammation. In general, to limit inflammatory processes in infectious or non-infectious systemic inflammatory responses, a compensatory anti-inflammatory response operates to maintain immune balance or terminate inflammation reactions [27]. If *Nnat* performs an anti-inflammatory function, its expression would be expected to be decreased to maintain normal inflammatory function under inflammatory conditions induced by stimuli. Thus, LPS treatment can reduce *Nnat* expression. However, *Nnat* expression may be increased to prevent prolonged inflammation, unlike acute inflammation. Thus, the extent to which *Nnat* performs its anti-inflammatory function in a normal state should be maintained to alleviate the prolonged inflammatory environment, such as that associated with obesity. Another gene has also been identified to show different responses to acute and chronic inflammation. The function of the NAD$^+$-dependent deacetylase SIRT1 depends on NAD$^+$ availability. In acute inflammation, when NAD$^+$ is available, active SIRT1 directly deacetylates targets such as NF-κB p65 and p53, followed by the suppression of inflammation. In contrast, in chronic inflammation, the limited availability of NAD$^+$ and reduced expression of SIRT1 allows for the activation of inflammation and leads to chronic inflammation [28]. Additional studies in diverse physiological environments should be conducted to evaluate this difference.

The NF-κB complex plays a key role in inflammatory signal transduction and consists of p65 and the IκB heterodimer [22, 29−33]. In general, inflammatory signals phosphorylate IκB, followed by degradation. The p65 freed from the IκB complex translocates to the nucleus, and leads to the transcriptional activation of target genes. The p65 is modified by phosphorylation, acetylation, prolyl isomerization, nitrosylation, and ubiquitination [34−36] and these modifications affect the activity of p65. It is known that the acetylation at K310 of p65 facilitates phosphorylation of p65, and the phospho-p65 recruits p300/CBP, which also acetylates at K314 and K315 of p65 for transcriptional activation [37, 38]. In the present study, although NNAT expression reduced NF-κB luciferase activity, no significant difference of p65 phosphorylation at

S536 was observed. It indicates that NNAT would affect other modifications besides phosphorylation. One possibility is that if NNAT inhibits recruitment or activity of p300/CBP, it can explain why NNAT represses NF-κB activity without inducing phosphorylation change. In addition, the phosphorylation of p65 occurs at various regions, including four sites (S205, T254, S276, and S281) on the N-terminal RHD, two (S311 and S316) on the linker region C terminal to the RHD, and five (T435, S468, T505, S529, and S536) on the C-terminal TAD [34]. Therefore, to determine whether NNAT affects phosphorylation of p65 at other sites would be valuable, since we examined only S536 phosphorylation (Fig. 5B).

Additionally, a previous study showed that the expression of NNAT in human aortic endothelial cells increased activation of the NF-κB transcription complex [23]. This may indicate that the ability of NNAT to regulate the NF-κB pathway is context-dependent or involves other extracellular signals in different organs. To evaluate these possibilities, additional well-designed and detailed experiments are needed.

In conclusion, this study determined that *Nnat* is highly expressed in the adipose tissue of obese model mice and likely exerts anti-inflammatory activity to alleviate the obesity-induced chronic inflammation condition. In addition, we observed that *Nnat* expression levels were decreased following acute inflammatory stimuli, and NNAT inhibits expression of the p65 subunit of NF-κB in adipocytes. This finding improves the understanding of the immune balance in the regulation of obesity-induced chronic inflammation, and may facilitate the development of therapeutic anti-inflammatory agents.

Acknowledgments

References

1. Kahn BB, Flier JS. 2000. Obesity and insulin resistance. *J. Clin. Invest.* **106:** 473-481.

2. Harvey AE, Lashinger LM, Hursting SD. 2011. The growing challenge of obesity and cancer: an inflammatory issue. *Ann. NY Acad. Sci.* **1229:** 45-52.

3. Basen-Engquist K, Chang M. 2011. Obesity and cancer risk: recent review and evidence. *Curr. Oncol. Rep.* **13:** 71-76.

4. Greenberg AS, Obin MS. 2006. Obesity and the role of

adipose tissue in inflammation and metabolism. *Am. J. Clin. Nutr.* **83:** 461S-465S.

5. Lumeng CN, Saltiel AR. 2011. Inflammatory links between obesity and metabolic disease. *J. Clin. Invest.* **121:** 2111-2117.

6. Hotamisligil GS. 2006. Inflammation and metabolic disorders. *Nature* **444:** 860-867.

7. Moller DE. 2000. Potential role of TNF-alpha in the pathogenesis of insulin resistance and type 2 diabetes. *Trends Endocrinol. Metab.* **11:** 212-217.

8. Panee J. 2012. Monocyte chemoattractant protein 1 (MCP-1) in obesity and diabetes. *Cytokine* **60:** 1-12.

9. Perreault M, Marette A. 2001. Targeted disruption of inducible nitric oxide synthase protects against obesity-linked insulin resistance in muscle. *Nat. Med.* **7:** 1138-1143.

10. Dou D, Joseph R. 1996. Cloning of human neuronatin gene and its localization to chromosome-20q 11.2-12: the deduced protein is a novel "proteolipid". *Brain Res.* **723:** 8-22.

11. Kagitani F, Kuroiwa Y, Wakana S, Shiroishi T, Miyoshi N, Kobayashi S, *et al.* 1997. Peg5/neuronatin is an imprinted gene located on sub-distal chromosome 2 in the mouse. *Nucleic Acids Res.* **25:** 3428-3432.

12. Joseph R, Dou D, Tsang W. 1995. Neuronatin mRNA: alternatively spliced forms of a novel brain-specific mammalian developmental gene. *Brain Res.* **690:** 92-98.

13. Pitale PM, Howse W, Gorbatyuk M. 2017. Neuronatin protein in health and disease. *J. Cell. Physiol.* **232:** 477-481.

14. Vrang N, Meyre D, Froguel P, Jelsing J, Tang-Christensen M, Vatin V, *et al.* 2010. The imprinted gene neuronatin is regulated by metabolic status and associated with obesity. *Obesity* **18:** 1289-1296.

15. Chu K, Tsai MJ. 2005. Neuronatin, a downstream target of BETA2/NeuroD1 in the pancreas, is involved in glucose-mediated insulin secretion. *Diabetes* **54:** 1064-1073.

16. Joe MK, Lee HJ, Suh YH, Han KL, Lim JH, Song J, *et al.* 2008. Crucial roles of neuronatin in insulin secretion and high glucose-induced apoptosis in pancreatic beta-cells. *Cell Signal.* **20:** 907-915.

17. Suh YH, Kim WH, Moon C, Hong YH, Eun SY, Lim JH, *et al.* 2005. Ectopic expression of neuronatin potentiates adipogenesis through enhanced phosphorylation of cAMP-response element-binding protein in 3T3-L1 cells. *Biochem. Biophys. Res. Commun.* **337:** 481-489.

18. Margetic S, Gazzola C, Pegg GG, Hill RA. 2002. Leptin: a review of its peripheral actions and interactions. *Int. J. Obes. Relat. Metab. Disord.* **26:** 1407-1433.

19. Klok MD, Jakobsdottir S, Drent ML. 2007. The role of leptin and ghrelin in the regulation of food intake and body weight in humans: a review. *Obes. Rev.* **8:** 21-34.

20. Berndt J, Kovacs P, Ruschke K, Kloting N, Fasshauer M, Schon MR, *et al.* 2007. Fatty acid synthase gene expression in human adipose tissue: association with obesity and type 2 diabetes. *Diabetologia* **50:** 1472-1480.

21. Krogh A, Larsson B, von Heijne G, Sonnhammer EL. 2001. Predicting transmembrane protein topology with a hidden Markov model: application to complete genomes. *J. Mol. Biol.* **305:** 567-580.

22. Tak PP, Firestein GS. 2001. NF-kappaB: a key role in inflammatory diseases. *J. Clin. Invest.* **107:** 7-11.

23. Mzhavia N, Yu S, Ikeda S, Chu TT, Goldberg I, Dansky HM. 2008. Neuronatin: a new inflammation gene expressed on the aortic endothelium of diabetic mice. *Diabetes* **57:** 2774-2783.

24. Weinberg MB, Utter MF. 1979. Effect of thyroid hormone on the turnover of rat liver pyruvate carboxylase and pyruvate dehydrogenase. *J. Biol. Chem.* **254:** 9492-9499.

25. Jitrapakdee S, St Maurice M, Rayment I, Cleland WW, Wallace JC, Attwood PV. 2008. Structure, mechanism and regulation of pyruvate carboxylase. *Biochem. J.* **413:** 369-387.

26. Jitrapakdee S, Gong Q, MacDonald MJ, Wallace JC. 1998. Regulation of rat pyruvate carboxylase gene expression by alternate promoters during development, in genetically obese rats and in insulin-secreting cells. Multiple transcripts with 5'-end heterogeneity modulate translation. *J. Biol. Chem.* **273:** 34422-34428.

27. Adib-Conquy M, Cavaillon JM. 2009. Compensatory anti-inflammatory response syndrome. *Thromb. Haemost.* **101:** 36-47.

28. Liu TF, McCall CE. 2013. Deacetylation by SIRT1 reprograms inflammation and cancer. *Genes Cancer* **4:** 135-147.

29. Zandi E, Rothwarf DM, Delhase M, Hayakawa M, Karin M. 1997. The IkappaB kinase complex (IKK) contains two kinase subunits, IKKalpha and IKKbeta, necessary for IkappaB phosphorylation and NF-kappaB activation. *Cell* **91:** 243-252.

30. Li QT, Verma IM. 2002. NF-kappa B regulation in the immune system. *Nat. Rev. Immunol.* **2:** 725-734.

31. Lawrence T. 2009. The nuclear factor NF-kappaB pathway in inflammation. *Cold Spring Harb. Perspect. Biol.* **1:** a001651.

32. Bonizzi G, Karin M. 2004. The two NF-kappaB activation pathways and their role in innate and adaptive immunity. *Trends Immunol.* **25:** 280-288.

33. Baker RG, Hayden MS, Ghosh S. 2011. NF-kappaB, inflammation, and metabolic disease. *Cell Metab.* **13:** 11-22.

34. Christian F, Smith EL, Carmody RJ. 2016. The regulation of NF-kappaB subunits by phosphorylation. *Cells* **5:** E12.

35. Chen L, Fischle W, Verdin E, Greene WC. 2001. Duration of nuclear NF-kappaB action regulated by reversible acetylation. *Science* **293:** 1653-1657.

36. Kiernan R, Bres V, Ng RW, Coudart MP, El Messaoudi S, Sardet C, *et al.* 2003. Post-activation turn-off of NF-kappa B-dependent transcription is regulated by acetylation of p65. *J. Biol. Chem.* **278:** 2758-2766.

37. Buerki C, Rothgiesser KM, Valovka T, Owen HR, Rehrauer H, Fey M, *et al.* 2008. Functional relevance of novel p300-mediated lysine 314 and 315 acetylation of RelA/p65. *Nucleic Acids Res.* **36:** 1665-1680.

38. Rothgiesser KM, Fey M, Hottiger MO. 2010. Acetylation of p65 at lysine 314 is important for late NF-kappaB-dependent gene expression. *BMC Genomics* **11:** 22.